World Academy of Science, Engineering and Technology
International Journal of Mechanical and Mechatronics Engineering
Vol:12, No:3, 2018

Theoretical Study on the Forced Vibration of One Degree of Freedom System, Equipped with Inerter, under Load-Type or Displacement-Type Excitation

Barenten Suciu

***Abstract*—**In this paper, a theoretical study on the forced vibration of one degree of freedom system equipped with inerter, working under load-type or displacement-type excitation, is presented. Differential equations of movement are solved under cosinusoidal excitation, and explicit relations for the magnitude, resonant magnitude, phase angle, resonant frequency, and critical frequency are obtained. Influence of the inertance and damping on these dynamic characteristics is clarified. From the obtained results, one concludes that the inerter increases the magnitude of vibration and the phase angle of the damped mechanical system. Moreover, the magnitude ratio and difference of phase angles are not depending on the actual type of excitation. Consequently, such kind of similitude allows for the comparison of various theoretical and experimental results, which can be broadly found in the literature.

***Keywords*—**One degree of freedom vibration, inerter, parallel connection, load-type excitation, displacement-type excitation.

I. Introduction

DESIGN process of hybrid and electrical vehicles requires analogies between the mechanical and electrical systems. Thus, the design method of the electro-mechanical equipment can be unified by associating to the force, velocity, spring, dashpot, inerter, kinetic energy, and potential energy of the mechanical network, the current, voltage, inductor, resistor, capacitor, electric energy, and magnetic energy of the electrical network [1]. On the other hand, similar to an inductor, which furnishes electro-magnetic coupling, the inerter provides inertial coupling into the mechanical system [2]. So, it seems that better understanding on the change in dynamical behavior of the mechanical network is required to properly define the electro-mechanical analogy.

Previous studies indicate that the inerter is able to change the natural frequencies of vibration [2], [3], to provide nonlinear and/or apparent negative stiffness effects [4], etc.

Recently, it was presented an extensive theoretical study on the free vibration of *one degree of freedom system* (1DOFS), consisted of a mass, which is suspended by an elastic element, connected in parallel with a dissipative element, and an inerter [5]. It was argued that inertance reduces the natural frequency, the damping ratio, and the logarithmic decrement of the system [5]. On the other hand, in the presence of the inerter, the amplitude of vibration was increased, this effect being generated by the larger kinetic energy, initially furnished into the system [5]. It was then advanced the idea to control the natural damped frequency of the mechanical network by using an inerter of adjustable inertance [5]. This feature appears as similar to the impedance control, well-known for the electrical network, in which case, a capacitor of adjustable capacitance is used [6]-[8]. However, in order to extend the range of practical applications, behavior of the 1DOFS, using an inerter, and working under forced vibration, should be thoroughly clarified.

Hence, in this work, the dynamic characteristics of 1DOFS, equipped with inerter, are theoretically investigated under the forced vibration produced by two types of excitations, and the influence of the inertance on the parameters of similitude is emphasized.

Barenten Suciu is with the Department of Intelligent Mechanical Engineering, Fukuoka Institute of Technology, Fukuoka, 811-0295 Japan (phone: +81-92-606-4348; fax: +81-92-606-0747; e-mail: suciu@fit.ac.jp).

II. Vibration Model of 1DOFS, Equipped with Inerter, and Working under Two Types of Excitations

A. Forced Damped Vibration under Load-Type Excitation

Fig. 1 shows the schematic view of the investigated 1DOFS, in the case of forced damped vibration produced by a load-type excitation. Mass element m is suspended by an elastic element (spring of constant k), linked in parallel with a dissipative element (dashpot of damping coefficient c) and an inerter of apparent mass, or so-called *inertance* b. Coordinate x is measured from the static equilibrium position of the mass.

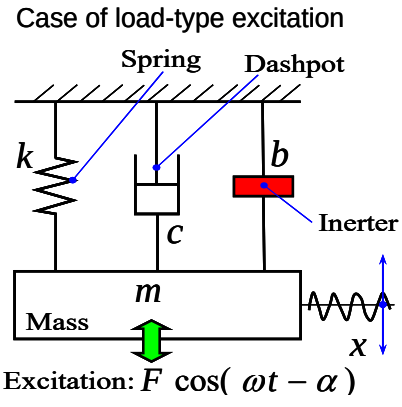

Fig. 1 Schematic view of the damped 1DOFS under load-type excitation, in which the mass element is suspended by an elastic element, connected in parallel with a dissipative element and an inerter

Mechanical energy is continuously supplied into the system by the cosinusoidal load-type excitation, and in such conditions, the so-called *forced damped vibration* is achieved.

For the 1DOFS from Fig. 1, in the absence of the inerter, the differential equation of movement can be written as [9]-[12]:

$$\begin{gathered} m\ddot{x} + c\dot{x} + kx = F\cos(\omega t - \alpha) \\ \Downarrow \\ \ddot{x} + 2\zeta_0\omega_{n,0}\dot{x} + \omega_{n,0}^2 x = \frac{F}{m}\cos(\omega t - \alpha) \end{gathered} \tag{1}$$

where the natural circular frequency $\omega_{n,0}$ and the damping ratio ζ_0 without inerter are given by:

$$\omega_{n,0} = \sqrt{k/m} \quad ; \quad \zeta_0 = 0.5c/\sqrt{km} \tag{2}$$

In the presence of the inerter, the differential equation of movement can be rewritten as:

$$\begin{gathered} (m+b)\ddot{x} + c\dot{x} + kx = F\cos(\omega t - \alpha) \\ \Downarrow \\ \ddot{x} + 2\zeta\omega_n\dot{x} + \omega_n^2 x = \frac{F}{m+b}\cos(\omega t - \alpha) \end{gathered} \tag{3}$$

where the natural circular frequency ω_n and the damping ratio ζ with inerter are given by [5]:

$$\begin{cases} \omega_n = \sqrt{k/(m+b)} = \omega_{n,0}/\sqrt{1+\lambda} \le \omega_{n,0} \\ \zeta = 0.5c/\sqrt{k(m+b)} = \zeta_0/\sqrt{1+\lambda} \le \zeta_0 \end{cases} \tag{4}$$

From (4), one ascertains that the inerter, of dimensionless inertance λ defined by (5), is able to reduce in the same manner both the natural frequency and the damping ratio of the 1DOFS (see also [5]).

$$\lambda = b/m \ge 0 \tag{5}$$

A solution that satisfies the differential equation (1) can be written as [8]-[12]:

$$x(t) = A_0\cos(\omega t - \alpha) + B_0\sin(\omega t - \alpha) \tag{6}$$

where the unknown constants A_0, B_0 can be obtained as:

$$\begin{cases} A_0 = \dfrac{F}{k}\dfrac{1-\overline{\omega}^2}{(1-\overline{\omega}^2)^2 + (2\zeta_0\overline{\omega})^2} \\ B_0 = \dfrac{F}{k}\dfrac{2\zeta_0\overline{\omega}}{(1-\overline{\omega}^2)^2 + (2\zeta_0\overline{\omega})^2} \end{cases} \tag{7}$$

in which the dimensionless circular frequency $\overline{\omega}$ is defined as:

$$\overline{\omega} = \omega/\omega_{n,0} \tag{8}$$

In such circumstances, the variation of elongation x versus time t, in the absence of the inerter, can be written as:

$$x(t) = X_0\cos(\omega t - \alpha - \Phi_0) \tag{9}$$

where X_0 is the amplitude:

$$X_0 = \frac{F/k}{\sqrt{(1-\overline{\omega}^2)^2 + (2\zeta_0\overline{\omega})^2}} \tag{10}$$

and Φ_0 is the phase angle:

$$\Phi_0 = \tan^{-1}\frac{2\zeta_0\overline{\omega}}{1-\overline{\omega}^2} \tag{11}$$

In order to evaluate the magnification factor of the amplitude X_0, relative to the static maximal elongation F/k, it is customarily to define the magnitude of vibration, as [9]-[12]:

$$M_0 = \frac{X_0 k}{F} = \frac{1}{\sqrt{(1-\overline{\omega}^2)^2 + (2\zeta_0\overline{\omega})^2}} \tag{12}$$

Resonant magnitude $M_{0,r}$ can be found from the condition $\partial M_0/\partial\overline{\omega} = 0$, which leads to the following expression for the dimensionless circular frequency at resonance:

$$\overline{\omega}_{0,r} = \sqrt{1-2\zeta_0^2} \tag{13}$$

From (13), one observes that the resonant peak is obtained only under the condition $0 \le \zeta_0 \le \sqrt{2}/2$, in which circumstances, the resonant magnitude can be calculated as:

$$M_{0,r} = \frac{1}{2\zeta_0\sqrt{1-\zeta_0^2}} \tag{14}$$

Results (13) and (14) are well-known in the literature [8]-[12]. However, it is useful to observe that a generalized expression, to estimate the resonant magnitude, can be written as:

$$M_{0,r} = \frac{1}{\sqrt{1-\overline{\omega}_{0,r}^4}} \tag{15}$$

Supplementary, a critical dimensionless circular frequency $\overline{\omega}_{0,cr}$, for which the unitary magnitude $M_0 = 1$ is achieved, can be defined and calculated as follows:

$$\overline{\omega}_{0,cr} = \sqrt{2(1-2\zeta_0^2)} = \sqrt{2}\overline{\omega}_{0,r} \tag{16}$$

Similarly, in the presence of the inerter into the 1DOFS, a solution that satisfies the differential equation (3) can be written as:

$$x(t) = A\cos(\omega t - \alpha) + B\sin(\omega t - \alpha) \tag{17}$$

where the unknown constants A, B can be obtained as:

$$\begin{cases} A = \dfrac{F}{k}\dfrac{1-(1+\lambda)\overline{\omega}^2}{[1-(1+\lambda)\overline{\omega}^2]^2 + (2\zeta_0\overline{\omega})^2} \\ B = \dfrac{F}{k}\dfrac{2\zeta_0\overline{\omega}}{[1-(1+\lambda)\overline{\omega}^2]^2 + (2\zeta_0\overline{\omega})^2} \end{cases} \tag{18}$$

Then, the variation of elongation x versus time t, in the presence of the inerter, can be written as:

$$x(t) = X\cos(\omega t - \alpha - \Phi) \tag{19}$$

where X is the amplitude:

$$X = \frac{F/k}{\sqrt{[1-(1+\lambda)\overline{\omega}^2]^2 + (2\zeta_0\overline{\omega})^2}} \tag{20}$$

and Φ is the phase angle:

$$\Phi = \tan^{-1}\frac{2\zeta_0\overline{\omega}}{1-(1+\lambda)\overline{\omega}^2} \tag{21}$$

Similar to (12), the magnitude of vibration can be defined as:

$$M = \frac{Xk}{F} = \frac{1}{\sqrt{[1-(1+\lambda)\overline{\omega}^2]^2 + (2\zeta_0\overline{\omega})^2}} \tag{22}$$

and then, the resonant magnitude M_r can be found from the condition $\partial M / \partial\overline{\omega} = 0$, which gives the following expression for the dimensionless circular frequency at resonance:

$$\overline{\omega}_r = \frac{\sqrt{1+\lambda-2\zeta_0^2}}{1+\lambda} \tag{23}$$

From (23), one observes that the resonant peak is obtained only under the condition $0 \le \zeta_0 \le \sqrt{2(1+\lambda)}/2$, which can be rewritten as $\lambda \ge 2\zeta_0^2 - 1$. In such circumstances, the resonant magnitude can be calculated as:

$$M_r = \frac{1+\lambda}{2\zeta_0\sqrt{1+\lambda-\zeta_0^2}} \tag{24}$$

Again, it is useful to observe that a generalized expression to estimate the resonant magnitude can be written as:

$$M_r = \frac{1}{\sqrt{1-(1+\lambda)^2\overline{\omega}_r^4}} \tag{25}$$

Moreover, the critical dimensionless circular frequency $\overline{\omega}_{cr}$, for which the unitary magnitude $M = 1$ is achieved, can be calculated as:

$$\overline{\omega}_{cr} = \frac{\sqrt{2(1+\lambda-2\zeta_0^2)}}{1+\lambda} = \sqrt{2}\overline{\omega}_r \tag{26}$$

which is a result similar to (16).

As expected, by imposing $\lambda = 0$ in the results (20)-(26), derived when the 1DOFS is furnished with inerter, one regains the results (10)-(16), obtained in the absence of the inerter.

In order to clarify the influence of inertance on the amplitude or magnitude of vibration, and on the phase angle, it is useful to define the amplitude ratio $\overline{X}$ or magnitude ratio $\overline{M}$, as:

$$\overline{X} = \frac{X}{X_0} = \overline{M} = \frac{M}{M_0} = \sqrt{\frac{(1-\overline{\omega}^2)^2 + (2\zeta_0\overline{\omega})^2}{[1-(1+\lambda)\overline{\omega}^2]^2 + (2\zeta_0\overline{\omega})^2}} \tag{27}$$

and also the difference of phase angles as:

$$\Phi - \Phi_0 = \tan^{-1}\frac{2\zeta_0\lambda\overline{\omega}^3}{(1+\lambda)\overline{\omega}^4 - (2+\lambda-4\zeta_0^2)\overline{\omega}^2 + 1} \ge 0 \tag{28}$$

From (28), one observes that inertance augments the phase angle of forced damped vibration under load-type excitation.

Since the partial derivative of the difference of phase angles versus λ is positive:

$$\frac{\partial(\Phi - \Phi_0)}{\partial\lambda} \ge 0 \tag{29}$$

one concludes that $\Phi - \Phi_0$ monotonically augments against the dimensionless inertance. On the other hand, since the partial derivative $\partial(\Phi - \Phi_0)/\partial\overline{\omega}$ becomes nil for:

$$\overline{\omega}_{opt}^2 = \frac{\sqrt{(2+\lambda-4\zeta_0^2)^2 + 12(1+\lambda)} - (2+\lambda-4\zeta_0^2)}{2(1+\lambda)} \tag{30}$$

a mountain shape graph is likely to be found for the difference of phase angles versus the dimensionless circular frequency, where the peak is attained for $\overline{\omega}_{opt}$ (see also Figs. 13-15).

B. Forced Damped Vibration under Displacement-type Excitation

Fig. 2 shows the schematic view of the investigated 1DOFS, in the case of forced damped vibration, which is generated by a displacement-type excitation. Compared to Fig. 1, the mass is not suspended, but supported by a suspension consisted of a spring, a dashpot, and an inerter, all connected in parallel.

For the 1DOFS from Fig. 2, in the absence of the inerter, the differential equation of motion can be written as [9]-[12]:

$$\begin{gathered} m\ddot{x} + c\dot{x} + kx = c\dot{y} + ky \\ \Downarrow \\ \ddot{x} + 2\zeta_0\omega_{n,0}\dot{x} + \omega_{n,0}^2 x = 2\zeta_0\omega_{n,0}\dot{y} + \omega_{n,0}^2 y \end{gathered} \tag{31}$$

where the excitation and the excitation velocity are given by:

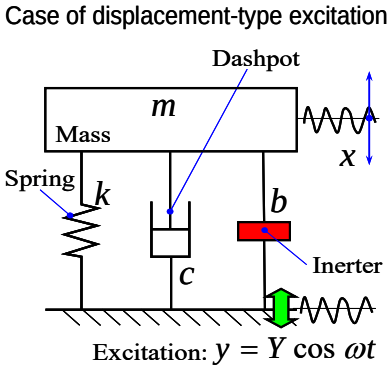

Fig. 2 Schematic view of the damped 1DOFS under displacement-type excitation, in which the mass element is supported by an elastic element, connected in parallel with a dissipative element and an inerter

$$y = Y\cos\omega t \quad ; \quad \dot{y} = -\omega Y\sin\omega t \tag{32}$$

By substituting (32) in the lower part of (31), the equation of motion can be rewritten as:

$$\ddot{x} + 2\zeta_0\omega_{n,0}\dot{x} + \omega_{n,0}^2 x = Y\omega_{n,0}(\omega_{n,0}\cos\omega t - 2\zeta_0\omega\sin\omega t) \tag{33}$$

In the presence of the inerter into the 1DOFS, similar to (3) and (31)-(33), the differential equation of movement can be written as follows:

$$\ddot{x} + 2\zeta\omega_n\dot{x} + \omega_n^2 x = Y\omega_n(\omega_n\cos\omega t - 2\zeta\omega\sin\omega t) \tag{34}$$

A solution that satisfies the equation of motion (33) can be written as:

$$x(t) = C_0\cos\omega t + D_0\sin\omega t \tag{35}$$

where the unknown constants C_0, D_0 can be obtained as:

$$\begin{cases} C_0 = Y\dfrac{1-(1-4\zeta_0^2)\overline{\omega}^2}{(1-\overline{\omega}^2)^2 + (2\zeta_0\overline{\omega})^2} \\ D_0 = Y\dfrac{2\zeta_0\overline{\omega}^3}{(1-\overline{\omega}^2)^2 + (2\zeta_0\overline{\omega})^2} \end{cases} \tag{36}$$

In such circumstances, the variation of elongation x versus time t, in the absence of the inerter, can be written as:

$$x(t) = X_0\cos(\omega t - \Phi_0) \tag{37}$$

where X_0 is the amplitude:

$$X_0 = Y\sqrt{\frac{1+(2\zeta_0\overline{\omega})^2}{(1-\overline{\omega}^2)^2 + (2\zeta_0\overline{\omega})^2}} \tag{38}$$

and Φ_0 is the phase angle:

$$\Phi_0 = \tan^{-1}\frac{2\zeta_0\overline{\omega}^3}{1-(1-4\zeta_0^2)\overline{\omega}^2} \tag{39}$$

In order to evaluate the magnification factor of the amplitude X_0, relative to the excitation amplitude Y, it is customarily to define the magnitude of vibration, as [8]-[12]:

$$M_0 = \frac{X_0}{Y} = \sqrt{\frac{1+(2\zeta_0\overline{\omega})^2}{(1-\overline{\omega}^2)^2 + (2\zeta_0\overline{\omega})^2}} \tag{40}$$

Resonant magnitude $M_{0,r}$ can be found from the condition $\partial M_0 / \partial\overline{\omega} = 0$, which leads to the following expression for the dimensionless circular frequency at resonance:

$$\overline{\omega}_{0,r}^2 = \frac{\sqrt{1+8\zeta_0^2}-1}{4\zeta_0^2} \tag{41}$$

From (41), one observes that the resonant peak is achieved for any value of the damping ratio in the domain of $0 \le \zeta_0 \le 1$. In these circumstances, the resonant magnitude can be calculated with the same general expression (15) found in the case of load- type excitation, as follows:

$$M_{0,r} = \frac{1}{\sqrt{1-\overline{\omega}_{0,r}^4}} \tag{42}$$

In the case of displacement-type excitation, the critical dimensionless circular frequency $\overline{\omega}_{0,cr}$ of the forced vibration, for which the unitary magnitude $M_0 = 1$ is achieved, can be calculated as:

$$\overline{\omega}_{0,cr} = \sqrt{2} \tag{43}$$

Thus, $\overline{\omega}_{0,cr}$ displays a constant value, regardless the amount of inertance and/or damping introduced into the 1DOFS. Similarly, in the presence of the inerter, a solution that satisfies the differential equation (34) can be written as:

$$x(t) = C\cos\omega t + D\sin\omega t \tag{44}$$

where the unknown constants C, D can be obtained as:

$$\begin{cases} C = Y\dfrac{1-(1+\lambda-4\zeta_0^2)\overline{\omega}^2}{[1-(1+\lambda)\overline{\omega}^2]^2 + (2\zeta_0\overline{\omega})^2} \\ D = Y\dfrac{2\zeta_0(1+\lambda)\overline{\omega}^3}{[1-(1+\lambda)\overline{\omega}^2]^2 + (2\zeta_0\overline{\omega})^2} \end{cases} \tag{45}$$

Then, the variation of elongation x versus time t, in the

presence of the inerter, can be written as:

$$x(t) = X\cos(\omega t - \Phi) \tag{46}$$

where X is the amplitude:

$$X = Y\sqrt{\frac{1+(2\zeta_0\overline{\omega})^2}{[1-(1+\lambda)\overline{\omega}^2]^2+(2\zeta_0\overline{\omega})^2}} \tag{47}$$

and Φ is the phase angle:

$$\Phi = \tan^{-1}\frac{2\zeta_0(1+\lambda)\overline{\omega}^3}{1-(1+\lambda-4\zeta_0^2)\overline{\omega}^2} \tag{48}$$

Similar to (40), the magnitude of vibration can be defined as:

$$M = \frac{X}{Y} = \sqrt{\frac{1+(2\zeta_0\overline{\omega})^2}{[1-(1+\lambda)\overline{\omega}^2]^2+(2\zeta_0\overline{\omega})^2}} \tag{49}$$

and then, the resonant magnitude M_r can be found from the condition $\partial M/\partial\overline{\omega} = 0$, which gives the following expression for the dimensionless circular frequency at resonance:

$$\overline{\omega}_r^2 = \frac{\sqrt{1+8\zeta_0^2/(1+\lambda)}-1}{4\zeta_0^2} \tag{50}$$

From (50), one observes that the resonant peak is obtained for any value of the damping ratio in the domain of $0 \le \zeta_0 \le 1$. In these circumstances, the resonant magnitude can be calculated with the same general expression (25), which was found in the case of load-type excitation, as follows:

$$M_r = \frac{1}{\sqrt{1-(1+\lambda)^2\overline{\omega}_r^4}} \tag{51}$$

For displacement-type excitation, in the presence of the inerter, the critical dimensionless circular frequency $\overline{\omega}_{cr}$ of the forced vibration, for which the unitary magnitude $M = 1$ is achieved, can be calculated as:

$$\overline{\omega}_{cr} = \sqrt{2/(1+\lambda)} \tag{52}$$

Compared to (43), expression (52) indicates that the critical frequency is not depending on the damping ratio, but it is decreasing at the augmentation of the dimensionless inertance.

As expected, by imposing $\lambda = 0$ in the results (47)-(52), attained when the 1DOFS is supplied with inerter, one regains the results (38)-(43), obtained in the absence of the inerter.

In order to clarify the influence of inertance on the amplitude or magnitude of vibration, and on the phase angle, it is useful to define the amplitude ratio $\overline{X}$ or magnitude ratio $\overline{M}$, as:

$$\overline{X} = \frac{X}{X_0} = \overline{M} = \frac{M}{M_0} = \sqrt{\frac{(1-\overline{\omega}^2)^2+(2\zeta_0\overline{\omega})^2}{[1-(1+\lambda)\overline{\omega}^2]^2+(2\zeta_0\overline{\omega})^2}} \tag{53}$$

and also the difference of phase angles as:

$$\Phi - \Phi_0 = \tan^{-1}\frac{2\zeta_0\lambda\overline{\omega}^3}{(1+\lambda)\overline{\omega}^4-(2+\lambda-4\zeta_0^2)\overline{\omega}^2+1} \ge 0 \tag{54}$$

These expressions coincide with the magnitude ratio (27) and the difference of phase angles (28), which were obtained above, for the case of load-type excitation.

In conclusion, for two different types of vibration tests, one performed under load-type excitation and the other under displacement-type excitation, the results obtained for the magnitude ratio and the difference of phase angles should be identical. Hence, these two parameters occur as similitude parameters between two different types of vibration tests conducted on the same 1DOFS, equipped with inerter. Based on this observation, suitable comparison can be carried out between various theoretical and experimental results, which are available in the extensive literature dedicated to the study of inerters and their dynamical effects.

III. Results and Discussions

A. Forced Damped Vibration under Load-Type Excitation

Fig. 3 shows the variation of the vibration magnitude versus the dimensionless circular frequency, obtained under load-type excitation in the absence of the inerter, for various values of the damping ratio $\zeta_0 =$ 0.01, 0.1, 0.2, 0.5, $\sqrt{2}/2$, and 1. Such well-known reference results [9]-[12], are used to emphasize below the dynamic effects produced by the presence of the inerter.

Fig. 4 shows the variation of the vibration magnitude versus the dimensionless circular frequency, obtained under load-type excitation for a dimensionless inertance of $\lambda = 2$, and for various values of the damping ratio. Compared to Fig. 3, the resonant peak appears as higher but narrower, and shifted toward smaller values of $\overline{\omega}$. Such change in the appearance of the resonant peak is produced by the reduction of damping ratio, predicted by (4), and by the reduction of resonant frequency, predicted by (23), at the augmentation of the inertance λ.

In order to better emphasize the alteration of the resonant peak, Fig. 5 illustrates the variation of the magnitude versus the dimensionless circular frequency, obtained under load-type excitation for a fixed value of the damping ratio $\zeta_0 = 0.1$, and for several values of the dimensionless inertance $\lambda =$ 0, 0.5, 1, 2, 3, and 10.

Concerning the position of the resonant peak, Fig. 6 shows the variation of dimensionless circular frequency at resonance $\overline{\omega}_r$ versus the dimensionless inertance, for various values of the damping ratio $\zeta_0 =$ 0, 0.3, 0.4, 0.5, 0.6, $\sqrt{2}/2$, 0.8, 0.9, and 1. In the absence of the inerter (see on Fig. 6 the vertical line corresponding to $\lambda = 0$), the resonant peak occurs only

under the condition $\zeta_0 \le \sqrt{2}/2$ (see also (13) and [9]-[12]). Similarly, in the presence of the inerter, resonant peak occurs only if the condition $\lambda \ge 2\zeta_0^2 - 1$ is satisfied (see (23) and Fig. 6 for $\zeta_0 = 0.8$, 0.9, and 1). For small damping ratios (e.g., 0, 0.3, 0.4, 0.5 on Fig. 6), the resonant peak is gradually shifted toward smaller values of $\overline{\omega}$, at the inertance augmentation. However, for larger damping ratios, the resonant peak is firstly shifted toward larger, and then, toward smaller values of $\overline{\omega}$, at the inertance augmentation. Hence, position control of the resonant peak can be achieved by proper adjustment of the inertance.

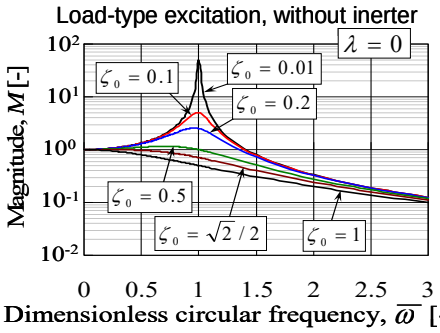

Fig. 3 Variation of the magnitude versus the dimensionless circular frequency, obtained under load-type excitation in the absence of the inerter, for various values of the damping ratio

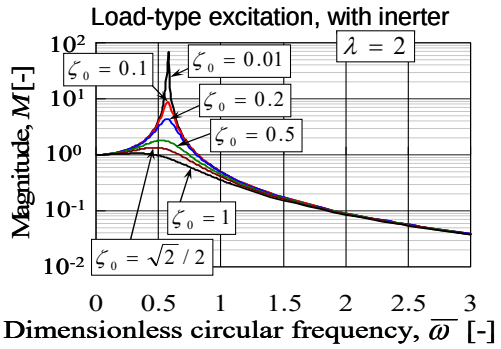

Fig. 4 Variation of the magnitude versus the dimensionless circular frequency, obtained under load-type excitation in the presence of the inerter, for various values of the damping ratio

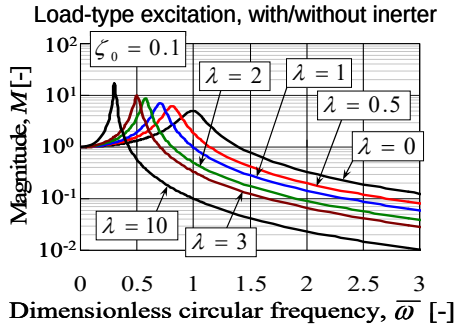

Fig. 5 Variation of the magnitude versus the dimensionless circular frequency, obtained under load-type excitation in the presence and absence of the inerter, for a fixed value of the damping ratio

Fig. 7 presents the variation of dimensionless circular critical frequency $\overline{\omega}_{cr}$ against the dimensionless inertance, for several values of the damping ratio.

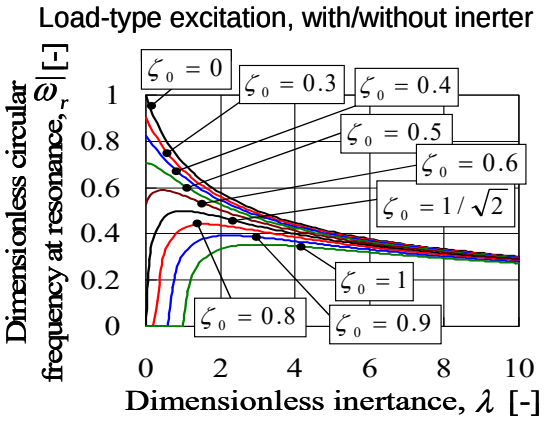

Fig. 6 Variation of the dimensionless circular frequency at resonance versus the dimensionless inertance, for various damping ratios

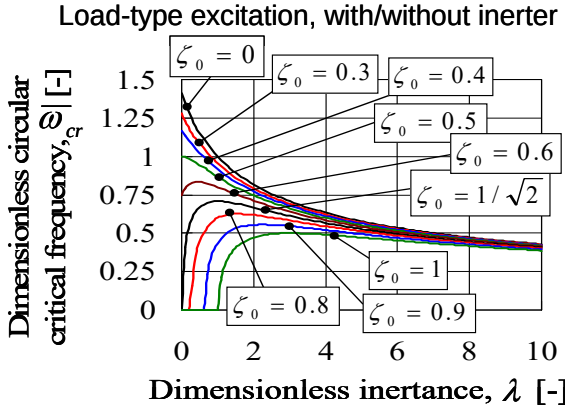

Fig. 7 Variation of the dimensionless circular critical frequency versus the dimensionless inertance, for various values of the damping ratio

Since, in the case of load-type excitation, the critical frequency can be obtained by simply multiplying the resonant frequency with a factor of $\sqrt{2}$ (see (16) and (26)), the shapes of the graphs shown by Fig. 7 and their interpretation are the same as for Fig. 6.

In order to complete the analysis concerning the magnitude of vibration, Figs. 8-9 illustrate the variation of the magnitude ratio versus the dimensionless circular frequency. Thus, in Fig. 8, the damping ratio is fixed to $\zeta_0 = 0.1$, and the dimensionless inertance is set to several values of $\lambda = 0$, 0.5, 1, 2, 3, and 10. On the other hand, in Fig. 9 the dimensionless inertance is fixed to $\lambda = 2$, and the damping ratio is set to various values. As already pointed out, same results are obtained for both load-type and displacement-type excitations (see (27) and (53)). For smaller frequencies a maximum, i.e. a resonant peak, and for larger frequencies a minimum, i.e. an anti-resonant peak, can be observed. As expected, height of these peaks increases at augmentation of the inertance but decreases at augmentation of the damping ratio.

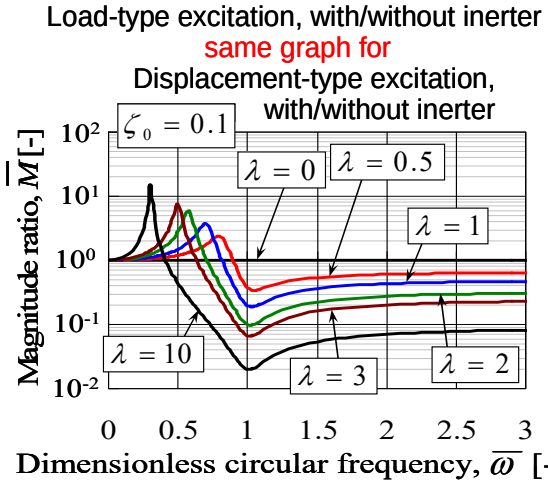

Fig. 8 Variation of the magnitude ratio versus the dimensionless circular frequency, for a fixed value of the damping ratio, and several values of the dimensionless inertance

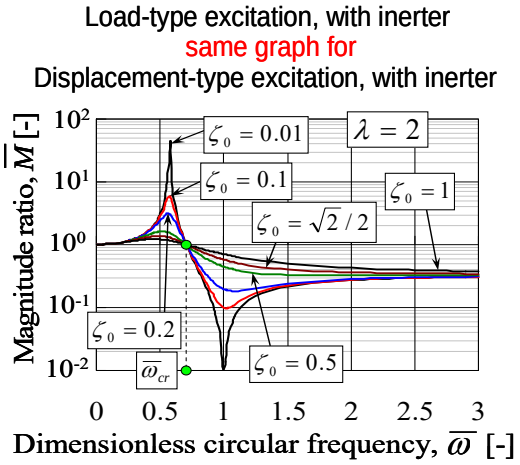

Fig. 9 Variation of the magnitude ratio versus the dimensionless circular frequency, for a fixed value of the dimensionless inertance, and several values of the damping ratio

Fig. 10 presents the variation of the phase angle versus the dimensionless circular frequency, obtained under load-type excitation in the absence of the inerter, for various values of the damping ratio. One notes that the phase angle increases against the dimensionless circular frequency, but the variation pattern is depending on the actual damping ratio. However, regardless the amount of damping, a phase angle of 90 degrees is attained for a dimensionless circular frequency of $\overline{\omega}_{0,\pi/2} = 1$ (see (11)), this corresponding to an inflexion point common to all curves. Although Fig. 10 is common knowledge [9]-[12], it is given here to easily distinguish the peculiar effects produced by the presence of the inerter into the mechanical system.

Thus, for comparison, Fig. 11 illustrates the variation of the phase angle versus the dimensionless circular frequency, found under load-type excitation in the presence of the inerter, for several values of the damping ratio.

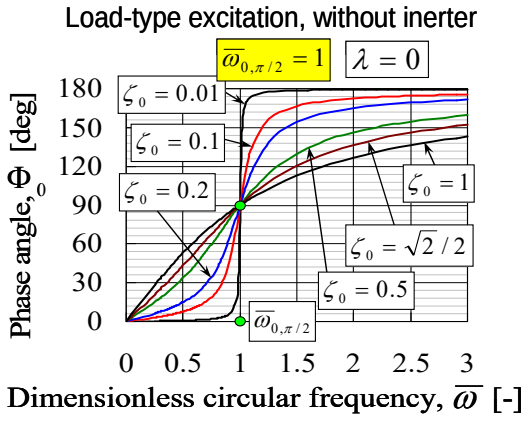

Fig. 10 Variation of the phase angle versus the dimensionless circular frequency, obtained under load-type excitation in the absence of the inerter, for various values of the damping ratio

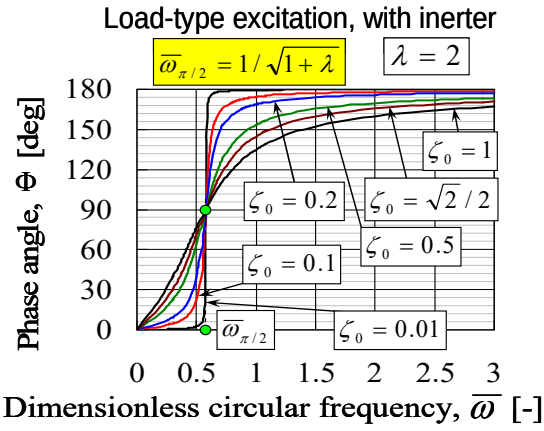

Fig. 11 Variation of the phase angle versus the dimensionless circular frequency, obtained under load-type excitation in the presence of the inerter, for various values of the damping ratio

Although the shapes of the curves from Fig. 11 are similar to those shown by Fig. 10, the inflexion point, common to all curves, occurs as shifted toward a smaller dimensionless circular frequency of $\overline{\omega}_{\pi/2} = 1/\sqrt{1+\lambda}$ (see also (21)).

In order to better understand the influence of inertance on the phase angle, Fig. 12 illustrates the variation of the phase angle against the dimensionless circular frequency, obtained under load-type excitation for a fixed value of the damping ratio $\zeta_0 = 0.1$, and for several values of the dimensionless inertance $\lambda = 0$, 0.5, 1, 2, 3, and 10. As expected from (28), for a given frequency and damping ratio, the phase angle increases at augmentation of the dimensionless inertance λ.

This phenomenon can be better perceived by analyzing the change in the difference of phase angles $\Phi - \Phi_0$. Thus, Fig. 13 presents the variation of the difference of phase angles found for $\lambda = 0.5$, 1, 2, 3, and 10, under a fixed damping ratio of $\zeta_0 = 0.5$. Additionally, Figs. 14-15 show the variation of the difference of phase angles calculated for $\zeta_0 = 0.01$, 0.1, 0.2, 0.5, $\sqrt{2}/2$, and 1, under a fixed value for the dimensionless

inertance.

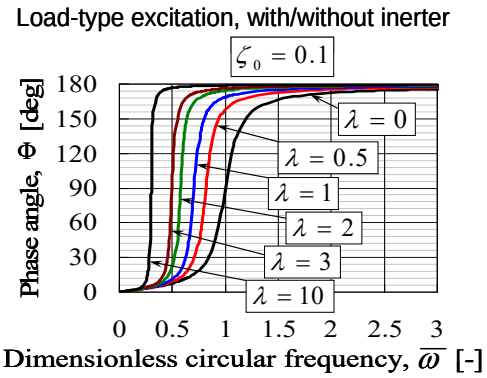

Fig. 12 Variation of the phase angle versus the dimensionless circular frequency, obtained under load-type excitation in the presence and absence of the inerter, for a fixed value of the damping ratio

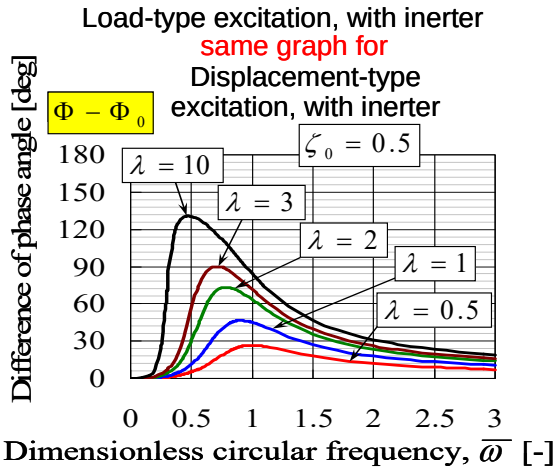

Fig. 13 Variation of the difference of phase angles versus the dimensionless circular frequency, for a fixed value of the damping ratio and various values of the dimensionless inertance

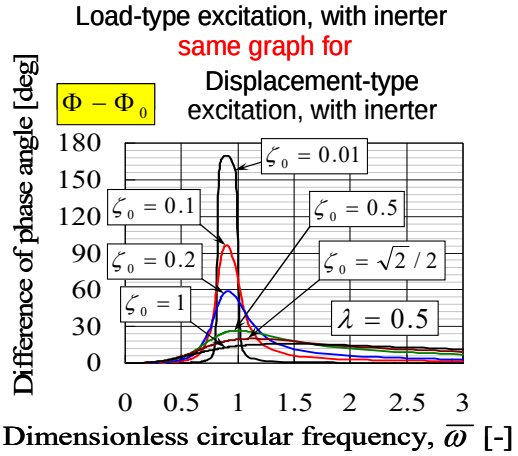

Fig. 14 Variation of the difference of phase angles versus the dimensionless circular frequency, for a fixed smaller value of the dimensionless inertance, and various values of the damping ratio

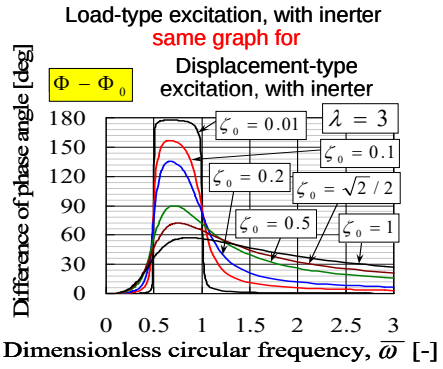

Fig. 15 Variation of the difference of phase angles versus the dimensionless circular frequency, for a fixed larger value of the dimensionless inertance, and various values of the damping ratio

Concretely, in Fig. 14, the dimensionless inertance is set to a smaller value of $\lambda = 0.5$, and in Fig. 15, to a larger value of $\lambda = 3$. All the curves shown by Figs. 13-15 display a mountain like shape against the dimensionless circular frequency. Height of the mountain peak increases at augmentation of the dimensionless inertance and reduction of the damping ratio. Higher inertance produces larger width of the peak, and also larger shift of the peak toward smaller frequencies.

B. Forced Damped Vibration under Displacement-Type Excitation

Fig. 16 presents the variation of the magnitude of vibration against the dimensionless circular frequency, obtained under displacement-type excitation in the absence of the inerter, for various values of the damping ratio $\zeta_0 = 0.01$, 0.1, 0.2, 0.5, $\sqrt{2}/2$, and 1. Such well-known reference results [9]-[12], are used to illustrate below the dynamic effects generated by the inerter. Thus, Fig. 17 presents the change of the magnitude of vibration versus the dimensionless circular frequency, obtained under displacement-type excitation for $\lambda = 2$, and for various values of the damping ratio. Compared to Fig. 16, the resonant peak appears as higher but narrower, and shifted toward smaller values of $\bar{\omega}$. Similar to the case of load-type excitation (see Figs. 3 and 4), such change in the appearance of the resonant peak is produced by the reduction of damping ratio, predicted by (4).

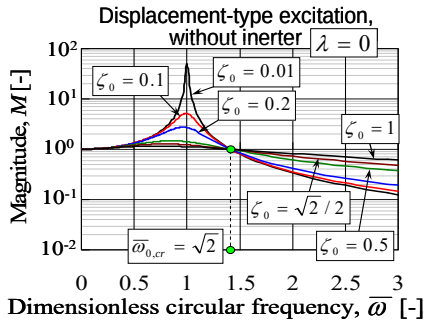

Fig. 16 Variation of the magnitude versus the dimensionless circular frequency, obtained under displacement-type excitation in the absence of the inerter, for various values of the damping ratio

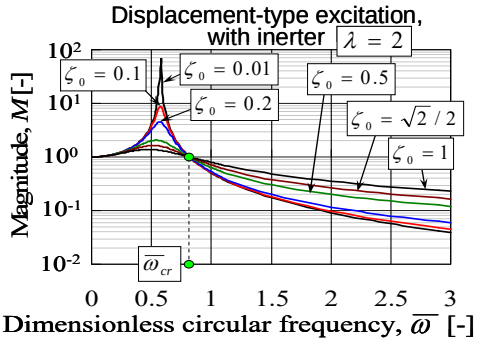

Fig. 17 Variation of the magnitude versus the dimensionless circular frequency, obtained under displacement-type excitation in the presence of the inerter, for various values of the damping ratio

Regardless the value of the damping ratio, curves from Figs. 16 or 17 share a common point that corresponds to the dimensionless critical circular frequency (see (43), (52)), and to the unitary magnitude. This common point appears as shifted toward smaller frequencies on Fig. 17, since the critical frequency $\overline{\omega}_{cr} = \sqrt{2/(1+\lambda)}$ is decreasing at the augmentation of the dimensionless inertance.

In order to better emphasize the change of the resonant peak, Fig. 18 illustrates the variation of the magnitude versus the dimensionless circular frequency, gained under displacement-type excitation for a fixed value of the damping ratio $\zeta_0 = 0.1$, and for several values of the dimensionless inertance $\lambda = 0$, 0.5, 1, 2, 3, and 10.

Concerning the location of the resonant peak, and position of the common critical point, Fig. 19 illustrates the variation of dimensionless circular frequency at resonance $\overline{\omega}_r$ and dimensionless circular critical frequency $\overline{\omega}_{cr}$ versus the dimensionless inertance, for various values of the damping ratio. As already mentioned, the resonant peak is achieved for any value of the damping ratio in the domain of $0 \le \zeta_0 \le 1$.

In contrast with the behavior observed for the load-type excitation (see Figs. 6-7), regardless the value of the damping ratio, the resonant and critical frequencies are invariantly shifted toward lower frequencies due to the presence of the inerter into the 1DOFS.

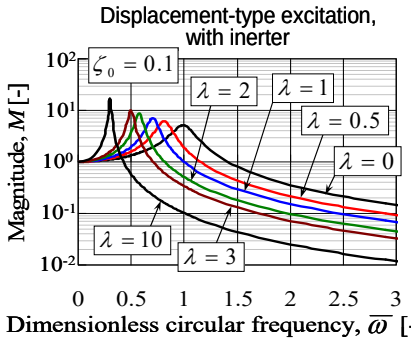

Fig. 18 Variation of the magnitude versus the dimensionless circular frequency, obtained under displacement-type excitation in the presence and absence of the inerter, for fixed damping ratio

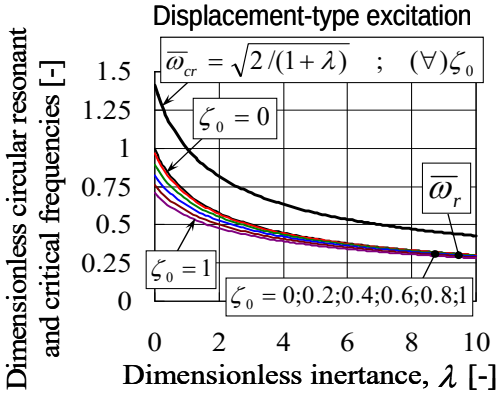

Fig. 19 Variation of the dimensionless circular frequency at resonance, and dimensionless circular critical frequency versus the dimensionless inertance, for various values of the damping ratios

Fig. 20 presents the variation of the phase angle versus the dimensionless circular frequency, obtained under displacement excitation in the absence of the inerter, for various values of the damping ratio $\zeta_0 = 0.01$, 0.1, 0.2, 0.5, $\sqrt{2}/2$, and 1. Such reference data [9]-[12], is necessary to discern below the peculiar effects produced by the presence of the inerter into the mechanical system.

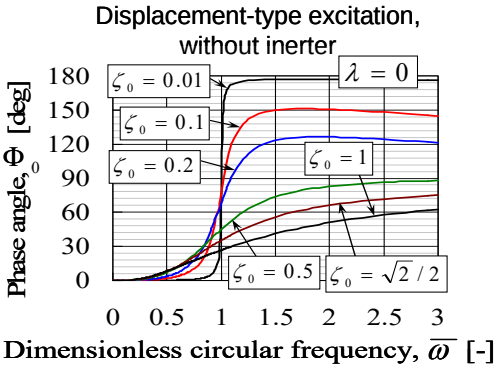

Fig. 20 Variation of the phase angle versus the dimensionless circular frequency, obtained under displacement-type excitation in the absence of the inerter, for various values of the damping ratio

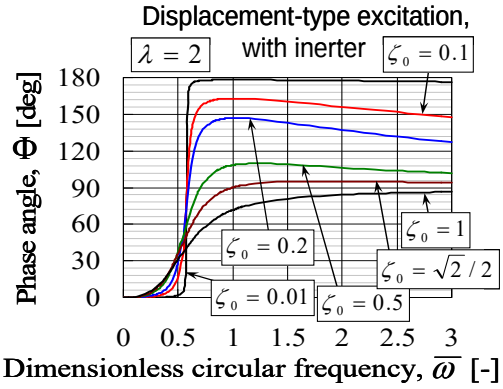

Fig. 21 Variation of the phase angle versus the dimensionless circular frequency, obtained under displacement-type excitation in the presence of the inerter, for various values of the damping ratio

Thus, for comparison, Fig. 21 presents the variation of the phase angle versus the dimensionless circular frequency, obtained under displacement-type excitation in the presence of the inerter, for the same values of the damping ratio as those used in Fig. 20.

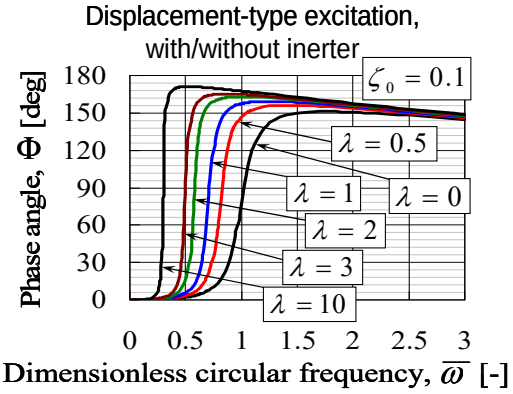

Fig. 22 Variation of the phase angle versus the dimensionless circular frequency, obtained under displacement-type excitation in the presence and absence of the inerter, for fixed damping ratio

Additionally, Fig. 22 illustrates the variation of the phase angle against the dimensionless circular frequency, obtained under displacement excitation for a fixed value of the damping ratio $\zeta_0 = 0.1$, and for several values of the dimensionless inertance $\lambda = 0$, 0.5, 1, 2, 3, and 10. As expected from (54), for a given frequency and damping ratio, the phase angle increases at the augmentation of the dimensionless inertance λ.

Although the variation pattern of the phase angle observed for the load-type excitation (monotonically increases against the dimensionless circular frequency, see Figs. 10-12) is different from the variation pattern noticed for the displacement-type excitation (see Figs. 20-22), the difference of phase angles (see (28), (54)) is not affected by the kind of excitation applied to the 1DOFS.

IV. Conclusions

From the theoretical investigation of the proposed 1DOFS, supplied with inerter and working under load-type or displacement-type excitation, the following conclusions can be drawn:

1) Regardless the kind of excitation applied to the studied 1DOFS, due to the reduction of the damping ratio at the augmentation of the inertance, the resonant peak appeared as higher but narrower, and with shifted location against the dimensionless circular frequency.
2) For displacement-type excitation, the shift of the resonant peak can be only toward smaller frequencies, but for load-type excitation, the resonant peak can be shifted both toward lower and higher frequencies. Thus, in the latter case, position control of the resonant peak can be achieved through the appropriate adjustment of the inertance.
3) Regardless the type of excitation considered, the phase angle increased at augmentation of the dimensionless inertance, or at reduction of the damping ratio.
4) Magnitude ratio and difference of phase angles displayed the same expressions, regardless the type of excitation. These two similitude parameters are unaffected by the type of vibration test conducted on the same 1DOFS, equipped with inerter. Using these parameters, proper comparison is possible between the various experimental and theoretical results, which are abundantly available in the literature regarding the dynamic behavior of inerters.
5) Magnitude ratio shows for smaller frequencies a resonant peak, and for larger frequencies an anti-resonant peak. Height of these peaks increases if the damping is reduced, and/or inertance is augmented.
6) Difference of phase angles displays a mountain like shape graph against the dimensionless circular frequency. Height of the mountain peak increases at augmentation of the inertance and/or reduction of the damping.

References

[1] M.C. Smith, "Synthesis of Mechanical Networks: The Inerter", *IEEE Transactions on Automatic Control*, 47(10), pp. 1648–1662, 2002.
[2] J. Yang, "Force Transmissibility and Vibration Power Flow Behaviour of Inerter-Based Vibration Isolators", *Journal of Physics: Conference Series* 744(012234), pp. 1–8, 2016.
[3] M.Z.Q. Chen, Y. Hu, L. Huang, and G. Chen, "Influence of Inerter on Natural Frequencies of Vibration Systems", *Journal of Sound and Vibration*, 333(7), pp. 1874–1887, 2014.
[4] J. Yang, Y.P. Xiong, and J.T. Xing, "Dynamics and Power Flow Behaviour of a Nonlinear Vibration Isolation System with a Negative Stiffness Mechanism", *Journal of Sound and Vibration*, 332(1), pp. 167–183, 2013.
[5] B. Suciu, and Y. Tsuji, "Theoretical Investigation on the Dynamic Characteristics of One Degree of Freedom Vibration System Equipped with Inerter of Variable Inertance", *International Journal of Mechanical, Aerospace, Industrial, Mechatronic and Manufacturing Engineering*, 11(3), pp. 414–422, 2017.
[6] F. A. Firestone, "A New Analogy between Mechanical and Electrical System Elements", *The Journal of the Acoustical Society of America*, 3, pp. 249–267, 1933.
[7] S. Darlington, "A History of Network Synthesis and Filter Theory for Circuits Composed of Resistors, Inductors, and Capacitors", *IEEE Transactions on Circuits and Systems*, 31, pp. 3–13, 1984.
[8] I. J. Busch-Vishniac, *Electromechanical Sensors and Actuators*. Berlin: Springer Science & Business Media, 1999.
[9] C.W. de Silva, *Vibration: Fundamentals and Practice*, London: CRC Press, 2nd ed., 2006.
[10] J.P. Den Hartog, *Mechanical Vibrations*. London: McGraw-Hill, 1940.
[11] D.J. Inman, and R.J. Singh, *Engineering Vibration*. New York: Prentice Hall, 2001.
[12] H. Benaroya, and M.L. Nagurka, *Mechanical Vibration: Analysis, Uncertainties, and Control*. London: CRC Press, 3rd ed., 2010.

Barenten Suciu was born on July 9, 1967. He received Dr. Eng. Degrees in the field of Mech. Eng. from the Polytechnic University of Bucharest, in 1997, and from the Kobe University, in 2003. He is working as Professor at the Department of Intelligent Mech. Eng., Fukuoka Institute of Technology. He is also entrusted with the function of Director of the Electronics Research Institute, affiliated to the Fukuoka Institute of Technology. He is member of JSME, JSAE, and JSASS. His major field of study is the tribological and dynamical design of various machine elements.